

1 A Rab GTPase protein FvSec4 is necessary for fumonisin B1 biosynthesis and virulence in
2 *Fusarium verticillioides*

3

4 Huijuan Yan, Jun Huang^a, Huan Zhang^b and Won Bo Shim *

5

6 ¹Department of Plant Pathology and Microbiology, Texas A&M University, College Station 77843,

7 TX, USA

8

9 Current affiliation;

10 ^a Department of Plant Pathology, Kansas State University, Manhattan, 66506, KS, USA

11 ^b Department of Biology, Texas A&M University, College Station 77843, TX, USA

12

13 * Corresponding author: Won Bo Shim, Email: wbshim@tamu.edu

14

15

16

17 **Abstract**

18

19 Rab GTPases are responsible for a variety of membrane trafficking and vesicular transportation in
20 fungi. But the role of Rab GTPases in *Fusarium verticillioides*, one of the key corn pathogens
21 worldwide, remains elusive. These Small GTPases in fungi, particularly those homologous to
22 *Saccharomyces cerevisiae* Sec4, are known to be associated with protein secretion, vesicular
23 trafficking, secondary metabolism and pathogenicity. Here, we characterized the molecular
24 functions of FvSec4 by generating a null mutant and learned that it is important for vegetative
25 growth, hyphal branching, and conidiation. Interestingly, the mutation did not impair the
26 expression of key conidiation-related genes. Meanwhile, the mutant did not show any defect in
27 sexual development, including perithecia production. GFP-FvSec4 localized to growing hyphal
28 tips, and raised the possibility that FvSec4 is involved in protein trafficking and endocytosis. The
29 mutant exhibited defect in corn stalk rot virulence and also significant alteration of fumonisin B1
30 production. The mutation led to more sensitivity to oxidative and cell wall stress agents, and
31 defects in carbon utilization. Gene complementation fully restored the defects in the mutant
32 demonstrating that FvSec4 plays important role in these functions. Taken together, our data
33 indicate that FvSec4 plays important roles in *F. verticillioides* hyphal development, virulence,
34 mycotoxin production and stresses response. Further study is needed to characterize whether the
35 mutation in FvSec4 leads to altered vesicle trafficking and protein secretion, which ultimately
36 impact *F. verticillioides* physiology and virulence.

37

38 **Key Words:** *Fusarium verticillioides*, Rab GTPase, Sec4, fumonisin B1, virulence

39 1. Introduction

40

41 Eukaryotic cells employ exocytosis and endocytosis to ensure proper cell physiology while
42 interacting with ambient environment ([Schultzhaus and Shaw 2015](#)). Vesicles mediate protein
43 transport during exo- and endocytosis ([Lazar, et al. 1997](#)), and Rab GTPases play important roles
44 in each transport step ([Lazar, et al. 1997](#)). This protein family, the largest subfamily of Ras
45 superfamily, is involved in vesicular trafficking regulation in eukaryotes by cycling between
46 inactive (GDP-bound) and active (GTP-bound) states ([Novick 2016](#)). In *Saccharomyces*
47 *cerevisiae*, 11 members of Rab GTPases have been identified and studied ([Lazar, et al. 1997](#)). Sec4
48 was first identified in *S. cerevisiae* which was shown to be involved in both secretory vesicles and
49 the plasma membrane ([Salminen and Novick 1987](#); [Goud, et al. 1988](#)). A recent study also
50 demonstrated that Sec4 is associated with the actin patches and endocytic internalization in yeast
51 ([Johansen, et al. 2016](#)).

52

53 In host-pathogen interactions, pathogenic fungi such as *Fusarium* species utilize many virulence
54 factors including cell-wall degrading enzymes, effectors and toxins by secreting these into the
55 extracellular space or the host cytoplasm to trigger a variety of responses in the host ([Ma, et al.](#)
56 [2013](#)). Thus, it is reasonable to anticipate that exocyst complex plays an important role in fungal
57 pathogenesis ([Chen, et al. 2015](#)). And Sec4 is a crucial component during this process which is
58 responsible for the transport of post-Golgi-derived secretory vesicles to the cell membrane
59 ([Salminen and Novick 1987](#)). In pathogenic fungi, a number of studies have shown that Sec4 is
60 associated with various cellular functions important for virulence. *CLPT1* in *Colletotrichum*
61 *lindemuthianum* was the first Sec4-like Rab GTPase gene reported in a phytopathogenic fungus
62 associated with intracellular vesicular trafficking ([Dumas, et al. 2001](#)). Later, *CLPT1* was further

63 demonstrated to be required for protein secretion and fungal pathogenicity ([Siriputthaiwan, et al.](#)
64 [2005](#)). In *Aspergillus fumigatus*, Sec4 homolog SrgA was shown to be involved in stress response,
65 virulence and phenotypic heterogeneity ([Powers-Fletcher, et al. 2013](#)). *Magnaporthe oryzae*
66 MoSec4 mutant exhibited defects in extracellular proteins secretion and consequently hyphal
67 development and pathogenicity in the rice blast fungus ([Zheng, et al. 2016](#)).

68
69 *Fusarium verticillioides* (teleomorph *Gibberella moniliformis* Wineland) is a fungal pathogen of
70 corn causing ear rot and stalk rot, posing significant food safety and security risks. The fungus is
71 a heterothallic ascomycete, but predominantly utilizes asexual spores, *i.e.* macroconidia and
72 microconidia, to rapidly reproduce on infected seeds and plant debris ([Leslie and Summerell](#)
73 [2008](#)). Most importantly, the fungus can produce various mycotoxins and biologically active
74 metabolites including fusaric acid, fusarins, and fumonisins on infested corn ears. Fumonisin B1
75 (FB1) is the most prevalent and toxic form of fumonisins, a group of polyketide-derived
76 mycotoxins structurally similar to sphinganine, and this mycotoxin is linked to devastating health
77 risks in humans and animals, including esophageal cancer and neural tube defect ([Alexander, et](#)
78 [al. 2009](#); [Wu, et al. 2014](#)). Fumonisin biosynthesis gene cluster, also referred to as the *FUM* cluster,
79 was first discovered by Proctor et al (1999). The cluster consists of a series of key genes encoding
80 biosynthetic enzymes and regulatory proteins ([Alexander, et al. 2009](#)), and molecular
81 characterization of *FUM1*, a polyketide synthase (PKS) gene, and *FUM8*, an aminotransferase
82 gene, showed their important roles in FB1 biosynthesis. FB1 production was significantly reduced
83 in *fum1* and *fum8* knockout mutants suggesting that these two key genes in the *FUM* cluster are
84 critical for fumonisin biosynthesis ([Proctor, et al. 1999](#); [Seo, et al. 2001](#)).

85
86 However, the regulatory mechanisms involved transport and secretion of FB1 in *F. verticillioides*

87 remain obscure. But it is reasonable to hypothesize that key mycotoxigenic fungi employ similar
88 mechanisms ([Woloshuk and Shim 2013](#)). A study performed in *Aspergillus parasiticus* described
89 how vesicles, not vacuoles, are primarily associated with aflatoxin biosynthesis and export
90 ([Chanda, et al. 2009](#)). The study also illustrated the development of mycotoxigenic vesicles under
91 conditions conducive to mycotoxin biosynthesis. A follow-up study also demonstrated that these
92 mycotoxigenic vesicles fuse with the cytoplasmic membrane to secrete and export aflatoxin
93 ([Chanda, et al. 2010](#)). Exocytosis relies on a exocyst complex which has eight proteins, including
94 Exo70p, Exo84p, Sec3p, Sec5p, Sec6p, Sec8p, Sec10p and Sec15p ([TerBush, et al. 1996](#); [Chen,](#)
95 [et al. 2015](#)). And Sec4 was recognized as the key component regulating the exocyst assembly
96 ([Guo, et al. 1999](#)). We hypothesize that Sec4-like Rab GTPases in *F. verticillioides* FB1 is
97 important for FB1 synthesis and transport. To test this, we identified a *S. cerevisiae* Sec4 homolog
98 FvSec4 and characterized its role in *F. verticillioides* vegetative growth, virulence and FB1
99 biosynthesis.

100

101 **2. Material and methods**

102

103 2.1 Fungal strains, culture media and growth conditions

104

105 *F. verticillioides* strain 7600 was used as the wild-type strains in this study ([Zhang, et al. 2018](#)).

106 All strains were grown and evaluated on V8 juice agar (200 ml of V8 juice, 3 g of CaCO₃ and 20

107 g of agar powder per liter), potato dextrose agar (PDA, Difco) and myro agar (1g of NH₄H₂PO₄, 3

108 g of KH₂PO₄, 2 g of MgSO₄·7H₂O, 5 g of NaCl, 40 g of sucrose and 20 g of agar powder per liter)

109 at room temperature for 8 days. For the spore production, 5 ml sterile water was added into 8 days

110 old V8 agar plates. Spore suspensions were harvested by passing through miracloth (EMD

111 Millipore) and counted using the hemocytometer. Newly harvested microconidia were suspended
112 in 0.2x potato dextrose broth (PDB) for 5h and 6.5 h with gentle shaking to assay spore
113 germinations. For genomic DNA extraction, strains were grown in YEPD liquid medium (3 g yeast
114 extract, 10 g peptone and 20 g dextrose per liter) at 25 °C in a rotatory shaker for 4 days. For stress
115 assays, strains were cultured on Czapek-Dox agar (2 g/L NaNO₃, 0.5 g/L MgSO₄-7H₂O, 0.5 g/L
116 KCl, 10 mg/L 14 FeSO₄-7H₂O, and 1 g/L K₂HPO₄, PH 7) amended with 70 mg/L Congo red, 2
117 mmol/L H₂O₂ or 0.01% SDS. For carbon utilization assay, 4 µl of 1 × 10⁶ conidial suspension was
118 inoculated on the center of Czapek-Dox agar plates with four different carbon sources, *i.e.* sucrose
119 (30 g/L), dextrose (10 g/L), fructose (10 g/L) and sorbitol(91 g/L), and incubating 8 days at room
120 temperature. For the mating study, conidia from wild-type, ΔFvsec4, ΔFvsec4-com strains were
121 harvested from culture grown on V8 agar for 7 days, and subsequently spread onto *F.*
122 *verticillioides* strain 7598, which was grown on carrot plates following our standard protocol
123 ([Sagaram and Shim 2007](#)).

124

125 2.2 Gene deletion and complementation, polymerase chain reaction (PCR), and transformation

126

127 The constructs for *F. verticillioides* transformation were generated following our laboratory
128 standard procedures ([Sagaram and Shim 2007](#)). Briefly, DNA fragments corresponding to 5' and
129 3' flanking regions of the gene were amplified from the wild-type genomic DNA. Meanwhile,
130 hygromycin B phosphotransferase (*HPH*) gene in pBP15 plasmid was used to obtain the HP and
131 PH fragments. 5' and 3' flanking region fragments were fused with PH and HP fragments by
132 single-joint PCR respectively ([Yu, et al. 2004](#); [Sagaram and Shim 2007](#)). We used protoplast
133 preparation and transformation protocols previous described in Zhang et al (2018). We used PCR
134 to verify targeted gene deletion mutations using primers OF/OR, UAF/YG/F, UAR/GE/R (Table

135 S1), followed by Southern blot and qPCR for further validation.

136

137 For gene complementation, wild-type *FvSEC4* gene with its native promoter was co-transformed
138 with a geneticin-resistant gene (*GEN*) into mutant protoplasts. All transformants were screened by
139 PCR. All primers used in this study are presented in Table S1. To construct the GFP-FvSec4
140 plasmid, *FvSEC4* coding region from *F. verticillioides* cDNA was amplified. *FvSEC4* native
141 promoter and terminator were amplified from wild-type DNA. GFP was amplified from PKNTG
142 plasmid (Dr. Wenhui Zheng, Fujian Agriculture and Forestry University, China). These four
143 purified products were introduced to the *HindIII* and *BamHI* sites of PKNTG using In-Fusion-HD
144 cloning kit (Takara Bio USA). The plasmid was then sequenced and introduced into the $\Delta Fvsec4$
145 strain for genetic complementation and localization study.

146

147 2.3 Nucleic acid manipulation and Southern blot

148

149 Bacterial plasmid DNA was isolated with Wizard miniprep DNA purification system (Promega).
150 Fungal genomic DNA isolation and Southern blot analysis were performed following standard
151 procedures ([Sambrook 2001](#)). Briefly, 10 μ g genomic DNA of each strain was completely digested
152 with *ClaI* and probed with a 32 P-labelled DNA fragment amplified from *F. verticillioides* genomic
153 DNA with primers FvAF1 and FvAR1 (Table S1).

154

155 2.4 Corn infection and fumonisin B1 assays

156

157 Infection assays on corn seedling were conducted as previously described with minor
158 modifications ([Kim, et al. 2018](#)). In this study, we used silver queen hybrid seeds (Burpee) for

159 seedling inoculation with fungal spore suspension. The seedlings were collected and analyzed after
160 a one-week growth period in the dark room. At least three biological and three technical replicates
161 were performed for each fungal strain.

162
163 For FB1 and ergosterol extraction, four silver queen seeds were surface sterilized using the method
164 previously described ([Christensen, et al. 2012](#)) with a minor modification. Sodium hypochlorite
165 (6%) was replaced with 10% bleach. Next, sterilized kernels were put on autoclaved 90-mm
166 Whatman filter paper. A scalpel was used to create wounds on the endosperm area, and these seeds
167 were placed in 40-ml borosilicate glass vials. Fungal spore suspensions (200 μ l, 10^7 /ml) were
168 inoculated into each vial, and these samples were incubated in room temperature for 7 days. FB1
169 extraction and sample purification methods were described previously ([Christensen, et al. 2012](#)).
170 HPLC analyses of FB1 and ergosterol were performed as described ([Shim and Woloshuk 1999](#)).
171 FB1 levels were then normalized to ergosterol contents. The experiment was repeated twice with
172 three biological replicates.

173
174 2.5 RNA extraction and gene expression study

175
176 A 1ml fungal spore suspension (10^6 spores/ml) was inoculated in 100 ml YEPD for 3 days at room
177 temperature with agitation (150 rpm). Then, mycelium from each flask was filtered through
178 Miracloth and weighed (0.3 g) before transferred to 100 ml myro liquid medium. Samples were
179 collected after 7 days incubation at room temperature with agitation (150 rpm). In addition, 2 ml
180 of spore suspension (10^6 spores/ml) were added into 100 ml YEPD, incubated for 20 h at 28°C at
181 150rpm before being harvested for RNA extraction for qPCR assay. Three replicates were
182 performed for each strain. Total RNA was extracted using Qiagen kit following the manufacturers'

183 protocols. RNA samples were converted into cDNA using the Verso cDNA synthesis kit (Thermo
184 Fisher Scientific), and qPCR analyses were performed with Step One plus real-time PCR system
185 using the DyNAmo ColorFlash SYBR Green qPCR Kit (Thermo Fisher Scientific) with 0.5
186 μ l cDNA as the template in per 10 μ l reaction. Expression levels were normalized with *F.*
187 *verticillioides* β -tubulin-encoding gene (FVEG_04081).

188

189 2.6 Microscopy and staining protocol

190

191 For hyphal growth imaging, strains were cultivated on 0.2xPDA for three days, and a block of agar
192 containing the growing edge (approximately 1 cm diameter) was cut and placed on a glass slide.
193 Next, water (10 μ l) was added on the agar block, and subsequently a coverslip was gently placed
194 on top. We incubated the sample at 28°C for additional 20 mins, and then observed hyphal growth
195 under a microscope (Olympus BX60). For GFP assay, we followed a previous method with minor
196 modifications ([Schultzhaus, et al. 2015](#)) and with assistance from Dr. Brian Shaw (Department of
197 Plant Pathology and Microbiology, TAMU). We used 16-18 h hypha to take images and water was
198 added on the top of agar. Samples were incubated at 28°C for 20 mins. For FM4-64 staining, 16-
199 18h growth of strains in 0.2xPDA were cut and put in the slide. Then, we added 10 μ l of 5 μ M
200 FM4-64 on top of medium and incubated at room temperature for 10 mins. We used 0.2xPDB
201 broth to wash samples twice before taking images. Images were prepared using ImageJ software
202 ([Schneider, et al. 2012](#)).

203

204 3. Results

205

206 3.1 Identification of the Sec4 homolog in *F. verticillioides*

207
208 We used the Sec4 protein sequence from the *S. cerevisiae* genome database
209 (<http://www.yeastgenome.org/>) to conduct a search into NCBI *F. verticillioides* database. This
210 search identified FVEG_06175 locus, a 990-bp gene encoding a putative 203-amino-acid protein,
211 which was designated as *FvSEC4* gene. To identify Sec4 homolog in other fungal species, the
212 predicted FvSec4 amino acid sequence from the *F. verticillioides* genome database was used for
213 our BLAST search. Multiple sequences alignment (Fig. 1) and phylogenetic analyses (Fig. S1A)
214 indicated that Sec4-like proteins share high amino acid identity in fungi, such as *S. cerevisiae* Sec4
215 (YFL005W, 64 % identity), *A. fumigatus* AfSrgA (Afu4g04810, 87% identity), *M. oryzae* MoSec4
216 (MGG_06135, 88% identity), *C. lindemuthianum* CLPT1 (AJ272025, 95% identity) and *C.*
217 *orbiculare* CoSec4 (Cob_13201, 95% identity). The predicted ScSec4 protein structure was
218 obtained from PDB (PDB ID: 1G16) and modified into alignment by ESPript ([Stroupe and](#)
219 [Brunger 2000](#); [Robert and Gouet 2014](#)).

220
221 3.2 Loss of FvSec4 impairs hyphal growth and conidiation

222
223 To investigate the function of FvSec4, we generated deletion mutants by replacing the entire gene
224 with a hygromycin-resistance marker (Fig. S2A). The gene-replacement mutants were confirmed
225 by Southern blot (Fig. S2B). The wild-type strain showed a 2.4-kb hybridizing band and all three
226 putative mutants had a 6.5-kb band, as expected when using the ORF 5' flanking probe for
227 Southern blot (Fig. S2B). These results suggested that the three mutant strains had a single-copy
228 insertion of the hygromycin-resistance marker and had no ectopic insertion events. We selected
229 the first mutant, which was designated $\Delta Fvsec4$, to perform further experiments, including qPCR
230 and phenotypic analyses in this study (Fig. S2C). We also generated a gene complementation strain

231 $\Delta Fvsec4$ -Com and a GFP-tagged complementation strain $\Delta Fvsec4$ -GFP-FvSec4.

232

233 To study the role of FvSec4 protein in *F. verticillioides* vegetative growth, we cultivated wild-
234 type, $\Delta Fvsec4$, $\Delta Fvsec4$ -Com and $\Delta Fvsec4$ -GFP-FvSec4 strains on V8, 0.2xPDA, myro agar
235 media. The $\Delta Fvsec4$ mutant showed a drastic reduction in growth and less fluffy mycelia on all
236 agar media tested. Both $\Delta Fvsec4$ -Com and $\Delta Fvsec4$ -GFP-FvSec4 strains exhibited full recovery
237 of growth defects (Fig. 2A). Moreover, $\Delta Fvsec4$ displayed hyphal hyperbranching under
238 microscopic examination (Fig. 2B). In addition, $\Delta Fvsec4$ mutant produced significantly lower
239 quantity of conidia when compared with wild-type and complemented strains (Fig. 3A). However,
240 conidia germination rate in the mutant and wild-type did not show a significant difference when
241 all strains were cultivated in 0.2xPDB liquid culture (Fig. 3B). Also, mycelial fresh weight did not
242 differ between wild-type and mutants after growing in YEPD liquid medium for 3 days (Fig. 3C).

243

244 To further characterize the basis for conidia production deficiency in $\Delta Fvsec4$, we used qPCR to
245 test transcription levels of key conidia regulation genes, including *BRLA*, *WETA*, *ABAA* and *STUA*.
246 Total RNA samples were extracted from strains cultured in myro broth for 7 days and in YEPD
247 broth for 20 h. The qPCR data suggested that conidia regulation genes are not impacted by the
248 FvSec4 deletion both in myro and YEPD culture, except *ABAA* expression that showed 40%
249 reduction when the mutant was cultured in myro broth (Fig. S3C and 3D). We also tested whether
250 FvSec4 is important for sexual reproduction, but all strains showed no defect perithecia production
251 (Fig. S3E).

252

253 3.3 Subcellular localization of FvSec4 suggests its role in vesicle trafficking

254

255 Since Sec4 is known as a key component that regulates the exocyst assembly, we studied the
256 localization of FvSec4 in *F. verticillioides*. We used the native promoter and fused GFP to the N-
257 terminus of *FvSEC4* coding sequence, and subsequently transformed the *FvSec4_{pro}-GFP-FvSec4*
258 construct into $\Delta Fvsec4$ strain. After confirming construct insertion through PCR, we performed a
259 live-cell imaging study of GFP-FvSec4 protein subcellular localization. The FvSec4 green
260 fluorescent signal accumulated mainly in the tips of hyphal, which was consistent with the
261 predicted Sec4 protein role in the tip vesicle transport and growth (Fig. 4A).

262
263 In addition to exocytosis, a previous study revealed that Sec4 is also important for endocytosis
264 ([Kean, et al. 1993](#)). To further test whether FvSec4 is associated with endocytosis, we stained the
265 mycelia of wild-type, $\Delta Fvsec4$, and $\Delta Fvsec4$ -Com with FM4-64, which is frequently used to study
266 endocytosis and vesicle trafficking in the fungal hyphae ([Fischer-Parton, et al. 2000](#)). Strong
267 fluorescent signals were detected in the Spitzenkörper region in both WT and $\Delta Fvsec4$ -Com, while
268 the $\Delta Fvsec4$ mutant showed a broader diffused staining at the mycelial tip. No Spitzenkörper
269 structure staining was observed in $\Delta Fvsec4$. This result suggests that $\Delta Fvsec4$ is either not properly
270 functioning in the uptake of FM4-64 or defective in recycling dyes to hyphal tip by exocytosis
271 (Fig. 4B).

272

273 3.4 FvSec4 is important for corn seedling rot virulence

274

275 To test whether FvSec4 plays a role in *F. verticillioides* virulence, we inoculated wild-type,
276 $\Delta Fvsec4$, $\Delta Fvsec4$ -Com spore suspensions, with sterilized distilled water as the negative control,
277 on one-week-old corn (silver queen hybrid) seedlings. After one week of incubation, we observed
278 significantly reduced rot symptoms in $\Delta Fvsec4$ mutant when compared to the wild-type strain (Fig.

279 5A and 5B). Gene complementation strain Δ Fvsec4-Com showed fully recovered stalk rot
280 symptoms in our assay. These results demonstrated that FvSec4 plays an important role in *F.*
281 *verticillioides* corn stalk rot virulence.

282

283 3.5 FvSec4 is essential for FB1 production

284

285 We tested FB1 production in *F. verticillioides* strains on both corn kernels (silver queen hybrid)
286 and in myro liquid medium after one-week incubation. The Δ Fvsec4 growth was reduced on corn
287 kernels but not in myro liquid medium (Fig. 6A and S3B). When FB1 production was normalized
288 to fungal growth, the results showed that Δ Fvsec4 produces dramatically lower levels of FB1 than
289 the wild-type progenitor in both growth conditions (Fig. 6B and 6C). To further understand how
290 FvSec4 impacts FB1 production at the molecular level, we used qPCR to study the expression of
291 two key FUM cluster genes *FUM1* and *FUM8*. RNA samples were collected from 7 day-post-
292 inoculation myro cultures. Both *FUM1* and *FUM8* expressions were significantly altered with
293 three-fold reduction in Δ Fvsec4 strain when compared to the wild-type and Δ Fvsec4-Com (Fig.
294 6D). Additionally, we also tested *SEC5*, *EXO70*, *SYN1* and *LCPI* gene expression in 7 day-post-
295 inoculation myro and 20h YEPD liquid media. Our data showed selected genes associated with
296 exocytosis were not altered but LCP1 transcription level was suppressed in the Δ Fvsec4 deletion
297 mutants (Fig. 6D and S3D). Taken together, our results indicate that FvSec4 is positively
298 associated with key *FUM* gene expression and ultimately FB1 production.

299

300 3.6 FvSec4 plays an important role in response to various stressors and extracellular enzymes
301 secretion

302

303 To investigate whether FvSec4 is involved in response to environment stress agents, we tested
304 vegetative growth of strains on minimal media amended with SDS (cell wall stress), Congo red
305 (cell wall stress) and H₂O₂ (oxidative stress) (Fig. 7A). The mutant growth rate was significantly
306 inhibited by these stress agents when compared to the wild-type strain, especially under the
307 oxidative stress with H₂O₂. (Fig. 7B). This outcome suggests that FvSec4 plays a role in response
308 to stress related to cell wall integrity and tolerance to oxidative stress.

309
310 To determine if FvSec4 is important for utilization of different carbon nutrients, we cultivated
311 wild-type, Δ Fvsec4, Δ Fvsec4-Com strains on Czapek-Dox agar medium containing different
312 carbon sources, *i.e.* sucrose, dextrose, fructose and sorbitol (Fig. 7C). We learned that the mycelial
313 growth of Δ Fvsec4 mutant exhibits significant restriction when grown on Czapek-Dox agar
314 containing dextrose or fructose but not sorbitol, when compared to the growth observed with
315 sucrose as the sole carbon source (Fig. 7D). Further studies are needed to determine if this
316 deficiency is due to carbon nutrient import into fungal cell or secretion defect in extracellular
317 catabolic enzymes.

318

319 **Discussion**

320

321 Exocytosis plays important roles in diverse functions such as cell polarization, growth,
322 morphology, and migration ([He and Guo 2009](#)). Exocytosis is responsible for the secretion of
323 cellular substances to the extracellular space. When pathogenic fungi colonize the living plants,
324 these organisms employ various strategies to adapt the host environment, namely by activating
325 signaling pathways associated with producing effectors, secondary metabolites and enzymes ([van
326 der Does and Rep 2017](#)). Previous studies indicate the Sec4 protein is a key regulator of multi-

327 subunit exocyst complex function ([Guo, et al. 1999](#)). Unlike in *S. cerevisiae* and *Candida albicans*,
328 Sec4 protein does not appear to be essential for viability but its function is critical for other
329 physiological functions in filamentous fungi ([Salminen and Novick 1987](#); [Mao, et al. 1999](#)). The
330 deletion of FvSec4, a highly conserved Rab GTPase protein, showed that this protein is essential
331 for the hyphal branching and growth, conidiation, stress responses and extracellular enzymes
332 secretion in *F. verticillioides*. FvSec4 was also indispensable for the virulence and mycotoxin
333 production.

334
335 Similar to Δ Mosec4 in *M. oryzae*, the virulence in Δ Fvsec4 strain was significantly reduced in our
336 seedling rot assay when compared with the wild-type progenitor. The reduced virulence in
337 Δ Mosec4 was partially due to appressoria abnormalities, particularly with lower turgor pressure
338 which is crucial for host penetration. Misshapen invasive hyphae and mislocalization of the
339 cytoplasmic effector in Δ Mosec4 mutant could have also negatively impacted virulence. Infection
340 structure such as appressoria are not recognized in *F. verticillioides*. But it is also noteworthy that
341 a mutation in a Sec4 homolog in wheat scab pathogen *F. graminearum*, a non-appressorium
342 producing ascomycete, also led to a virulence defect ([Zheng, et al. 2015](#)). Furthermore, the deletion
343 of Sec4 homolog BcSas1 in *Botrytis cinerea* also showed reduced virulence, and this outcome
344 could perhaps be explained by reduced growth rate and inadequate secretion of cell wall degrading
345 enzymes ([Zhang, et al. 2014](#)). While we cannot exclude slower vegetative growth as one of the
346 factors for reduced virulence, we can also propose that FvSec4 is involved in regulating the
347 expression of *F. verticillioides* secreted proteins. Consistent with this idea, we learned that the
348 expression of *FvLCPI* gene was significantly decreased in Δ Fvsec4. In our previous study, we
349 characterized FvLcp1 as a secreted protein that is involved host defense suppression and FB1
350 biosynthesis ([Zhang, et al. 2017](#)).

351
352 Another possible reason for attenuated pathogenicity is due to the mutant exhibiting deficiencies
353 in responding to various exogenously applied stress agents. In our study, $\Delta Fvsec4$ showed
354 increased sensitivity to H_2O_2 . It is well studied that reactive oxygen species (ROS) are accumulated
355 in plant hosts as a response to biotic and abiotic stress, and *Fusarium* species are directly causing
356 biotic stress on corn ([Lehmann, et al. 2015](#)). However, there are contradicting studies that suggest
357 ROS sensitivity may not be a key factor in fungal virulence. For instance, *B. cinerea* BcSas1
358 deletion mutants showed less sensitivity when compared to the wild-type ([Zhang, et al. 2014](#)). In
359 addition to ROS response, $\Delta Fvsec4$ exhibited growth deficiencies when utilizing different carbon
360 sources such as dextrose and fructose when compared to sucrose. This result raises a question
361 whether FvSec4 is involved in secretion of enzymes important for specific carbon nutrient
362 utilization. The hypersensitivity to H_2O_2 and the impairment in carbon nutrient utilization are
363 consistent with the attenuated virulence in $\Delta Fvsec4$. Published studies show that Sec4 Rab GTPase
364 are important for stress response and nutrient utilization ([Zhang, et al. 2014](#); [Zheng, et al. 2016](#)).
365 But, whether these two physiological processes are genetically linked needs further investigation.
366
367 Secondary metabolites are not required for conventional growth in *Fusarium* species but may offer
368 advantages in certain circumstances ([Ma, et al. 2013](#)). However, it is clear that mycotoxins
369 produced by fungi have adverse effects on human health and food safety ([Wu, et al. 2014](#)). There
370 is an earlier study by Zheng et al (2015) describing how Rab GTPase FgRab8 and exocytosis are
371 positively associated with *F. graminearum* mycotoxin DON production ([Zheng, et al. 2015](#)).
372 While DON has been recognized as a virulence factor in *F. graminearum*, FB1 is not a critical
373 factor for plant pathogenesis in *F. verticillioides* ([Proctor, et al. 1995](#); [Desjardins, et al. 2002](#)). In
374 this study, $\Delta Fvsec4$ showed a significantly lower levels of FB1 production when compared to the

375 wild-type strain, implying that this protein is critical for regulating mycotoxin biosynthesis. To
376 further understand how FvSec4 is impacting FB1 production, we tested the expression of key FUM
377 genes *FUM1* and *FUM8*. Our qPCR result showed that transcriptional expression of these two
378 FUM genes were significantly suppressed in the mutant. It is reasonable to hypothesize that this
379 Rab GTPase indirectly regulate transcriptional activities of FUM cluster through other
380 transcription factors.

381
382 Sec4 protein is known to control exocyst assembly and involved in secretion of vesicles. We
383 confirmed that FvSec4 is localized to the hyphal tip area which is consistent with the exocytosis
384 function. To investigate the role of FvSec4 in regulating the exocyst complex and other
385 downstream components, we identified three Sec4 downstream genes, *EXO70*, *SEC5* and *SYN1*,
386 to study their gene expression levels. We found that $\Delta Fvsec4$ mutation is not crucial for exocyst-
387 related gene expression except for *SEC5*, which showed 22% less expression when compared to
388 wild-type progenitor after a 7-day incubation in myro medium. This outcome led us to conclude
389 that Sec4 is not directly involved in the transcriptional regulation of its downstream genes
390 associated with exocytosis.

391
392 Spitzenkörper is a subcellular structure found at the fungal hyphal tip that is associated with polar
393 growth ([Riquelme and Sanchez-Leon 2014](#)). A previous report also indicated that Spitzenkörper
394 acts as a Vesicle Supply Center (VSC) where vesicles accumulate before being released to
395 extracellular space ([Bartnicki-Garcia, et al. 1989](#)). We stained mycelia with FM4-64, and the result
396 showed that our wild-type strain harbors a recognizable Spitzenkörper at the hyphal tip. However,
397 $\Delta Fvsec4$ exhibited accumulated fluorescence in both apical and subapical areas while the
398 Spitzenkörper was absent after the same staining treatment. When we consider the important role

399 of Spitzenkörper in delivering cell wall components to the sites of cell wall synthesis, perhaps this
400 abnormal Spitzenkörper structure and distribution are impacting the response to SDS and congo
401 red cell wall stress agents in $\Delta Fvsec4$ ([Riquelme 2013](#)). The lack of Spitzenkörper is possibly due
402 to $\Delta Fvsec4$ showing a defect in maintaining the balance between exocytosis and endocytosis. We
403 can further hypothesize that in the mutant insufficient number of vesicles are delivered to the
404 hyphal tip, and perhaps this leads to a significantly slower vegetative growth and hyper-branching.

405

406 **Acknowledgements**

407

408 We thank Dr. Brian Shaw, Ms. Blake Commer and Mr. Joe Vasselli (Department of Plant
409 Pathology and Microbiology, Texas A&M University) for help and discussion in microscopy. This
410 research was supported in part by the Agriculture and Food Research Initiative Competitive Grants
411 Program Grant (2013-68004-20359) from the USDA National Institute of Food and Agriculture.
412 The authors declare no conflict of interest.

413 **References**

414

415 Alexander NJ, Proctor RH, McCormick SP. 2009. Genes, gene clusters, and biosynthesis of
416 trichothecenes and fumonisins in *Fusarium*. *Toxin reviews* 28:198-215.

417 Bartnicki-Garcia S, Hergert F, Gierz G. 1989. Computer simulation of fungal morphogenesis and
418 the mathematical basis for hyphal (tip) growth. *Protoplasma* 153:46-57.

419 Chanda A, Roze LV, Kang S, Artymovich KA, Hicks GR, Raikhel NV, Calvo AM, Linz JE. 2009.
420 A key role for vesicles in fungal secondary metabolism. *Proc Natl Acad Sci U S A*
421 106:19533-19538.

422 Chanda A, Roze LV, Linz JE. 2010. A possible role for exocytosis in aflatoxin export in *Aspergillus*
423 *parasiticus*. *Eukaryot Cell* 9:1724-1727.

424 Chen X, Ebbole DJ, Wang Z. 2015. The exocyst complex: delivery hub for morphogenesis and
425 pathogenesis in filamentous fungi. *Curr Opin Plant Biol* 28:48-54.

426 Christensen S, Borrego E, Shim WB, Isakeit T, Kolomiets M. 2012. Quantification of fungal
427 colonization, sporogenesis, and production of mycotoxins using kernel bioassays. *J Vis*
428 *Exp.* 62: e3727.

429 Desjardins AE, Munkvold GP, Plattner RD, Proctor RH. 2002. FUM1-a gene required for
430 fumonisin biosynthesis but not for maize ear rot and ear infection by *Gibberella*
431 *moniliformis* in field tests. *Mol Plant Microbe Interact* 15:1157-1164.

432 Dumas B, Borel C, Herbert C, Maury J, Jacquet C, Balsse R, Esquerre-Tugaye MT. 2001.
433 Molecular characterization of CLPT1, a SEC4-like Rab/GTPase of the phytopathogenic
434 fungus *Colletotrichum lindemuthianum* which is regulated by the carbon source. *Gene*
435 272:219-225.

436 Fischer-Parton S, Parton RM, Hickey PC, Dijksterhuis J, Atkinson HA, Read ND. 2000. Confocal
437 microscopy of FM4-64 as a tool for analysing endocytosis and vesicle trafficking in living
438 fungal hyphae. *J Microsc* 198:246-259.

439 Goud B, Salminen A, Walworth NC, Novick PJ. 1988. A GTP-binding protein required for
440 secretion rapidly associates with secretory vesicles and the plasma-membrane in yeast. *Cell*
441 53:753-768.

442 Guo W, Roth D, Walch-Solimena C, Novick P. 1999. The exocyst is an effector for Sec4p, targeting
443 secretory vesicles to sites of exocytosis. *EMBO J* 18:1071-1080.

444

445

446
447 He B, Guo W. 2009. The exocyst complex in polarized exocytosis. *Current Opinion in Cell Biology*
448 21:537-542.

449 Johansen J, Alfaro G, Beh CT. 2016. Polarized Exocytosis Induces Compensatory Endocytosis by
450 Sec4p-Regulated Cortical Actin Polymerization. *PLoS Biol* 14:e1002534.

451 Kean LS, Fuller RS, Nichols JW. 1993. Retrograde lipid traffic in yeast: identification of two
452 distinct pathways for internalization of fluorescent-labeled phosphatidylcholine from the
453 plasma membrane. *J Cell Biol* 123:1403-1419.

454 Kim MS, Zhang H, Yan H, Yoon B-J, Shim WB. 2018. Characterizing co-expression networks
455 underpinning maize stalk rot virulence in *Fusarium verticillioides* through computational
456 subnetwork module analyses. *Scientific Reports* 8:8310.

457 Lazar T, Gotte M, Gallwitz D. 1997. Vesicular transport: how many Ypt/Rab-GTPases make a
458 eukaryotic cell? *Trends Biochem Sci* 22:468-472.

459 Lehmann S, Serrano M, L'Haridon F, Tjamos SE, Metraux JP. 2015. Reactive oxygen species and
460 plant resistance to fungal pathogens. *Phytochemistry* 112:54-62.

461 Leslie JF, Summerell BA. 2008. *The Fusarium laboratory manual*: John Wiley & Sons.

462 Ma LJ, Geiser DM, Proctor RH, Rooney AP, O'Donnell K, Trail F, Gardiner DM, Manners JM,
463 Kazan K. 2013. *Fusarium pathogenomics*. *Annu Rev Microbiol* 67:399-416.

464 Mao YX, Kalb VF, Wong B. 1999. Overexpression of a dominant-negative allele of SEC4 inhibits
465 growth and protein secretion in *Candida albicans*. *Journal of Bacteriology* 181:7235-7242.

466 Novick P. 2016. Regulation of membrane traffic by Rab GEF and GAP cascades. *Small GTPases*
467 7:252-256.

468 Powers-Fletcher MV, Feng X, Krishnan K, Askew DS. 2013. Deletion of the sec4 Homolog srgA
469 from *Aspergillus fumigatus* is associated with an impaired stress response, attenuated
470 virulence and phenotypic heterogeneity. *PLoS One* 8: e66741.

471 Proctor RH, Desjardins AE, Plattner RD, Hohn TM. 1999. A polyketide synthase gene required
472 for biosynthesis of fumonisin mycotoxins in *Gibberella fujikuroi* mating population A.
473 *Fungal Genet Biol* 27:100-112.

474 Proctor RH, Hohn TM, McCormick SP. 1995. Reduced virulence of *Gibberella zeae* caused by
475 disruption of a trichothecene toxin biosynthetic gene. *Mol Plant Microbe Interact* 8:593-
476 601.

477

- 478
479 Riquelme M. 2013. Tip Growth in Filamentous Fungi: A Road Trip to the Apex. In: Gottesman S,
480 editor. Annual Review of Microbiology, Vol 67. p. 587-609.
- 481 Riquelme M, Sanchez-Leon E. 2014. The Spitzenkorper: a choreographer of fungal growth and
482 morphogenesis. Current Opinion in Microbiology 20:27-33.
- 483 Robert X, Gouet P. 2014. Deciphering key features in protein structures with the new ENDscript
484 server. Nucleic Acids Res 42:W320-324.
- 485 Sagaram US, Shim WB. 2007. *Fusarium verticillioides* GBB1, a gene encoding heterotrimeric G
486 protein beta subunit, is associated with fumonisin B biosynthesis and hyphal development
487 but not with fungal virulence. Mol Plant Pathol 8:375-384.
- 488 Salminen A, Novick PJ. 1987. A ras-like protein is required for a post-golgi event in yeast secretion.
489 Cell 49:527-538.
- 490 Sambrook JaR, D. W. 2001. Molecular cloning : a laboratory manual. Cold Spring Harbor, N.Y.:
491 Cold Spring Harbor Laboratory press.
- 492 Schneider CA, Rasband WS, Eliceiri KW. 2012. NIH Image to ImageJ: 25 years of image analysis.
493 Nat Methods 9:671-675.
- 494 Schultzhaus Z, Yan H, Shaw BD. 2015. Aspergillus nidulans flippase DnfA is cargo of the
495 endocytic collar and plays complementary roles in growth and phosphatidylserine
496 asymmetry with another flippase, DnfB. Mol Microbiol 97:18-32.
- 497 Schultzhaus ZS, Shaw BD. 2015. Endocytosis and exocytosis in hyphal growth. Fungal Biology
498 Reviews 29:43-53.
- 499 Seo JA, Proctor RH, Plattner RD. 2001. Characterization of four clustered and coregulated genes
500 associated with fumonisin biosynthesis in *Fusarium verticillioides*. Fungal Genet Biol
501 34:155-165.
- 502 Shim WB, Woloshuk CP. 1999. Nitrogen repression of fumonisin B1 biosynthesis in *Gibberella*
503 *fujikuroi*. FEMS Microbiol Lett 177:109-116.
- 504 Siriputthaiwan P, Jauneau A, Herbert C, Garcin D, Dumas B. 2005. Functional analysis of CLPT1,
505 a Rab/GTPase required for protein secretion and pathogenesis in the plant fungal pathogen
506 *Colletotrichum lindemuthianum*. Journal of Cell Science 118:323-329.
- 507 Stroupe C, Brunger AT. 2000. Crystal structures of a Rab protein in its inactive and active
508 conformations. J Mol Biol 304:585-598.

- 509 TerBush DR, Maurice T, Roth D, Novick P. 1996. The Exocyst is a multiprotein complex required
510 for exocytosis in *Saccharomyces cerevisiae*. *EMBO Journal* 15:6483-6494.
- 511 van der Does HC, Rep M. 2017. Adaptation to the host environment by plant-pathogenic fungi.
512 *Annual Review of Phytopathology* 55:427-450.
- 513 Woloshuk CP, Shim WB. 2013. Aflatoxins, fumonisins, and trichothecenes: a convergence of
514 knowledge. *FEMS Microbiol Rev* 37:94-109.
- 515 Wu F, Groopman JD, Pestka JJ. 2014. Public health impacts of foodborne mycotoxins. *Annu Rev*
516 *Food Sci Technol* 5:351-372.
- 517 Yu JH, Hamari Z, Han KH, Seo JA, Reyes-Dominguez Y, Scazzocchio C. 2004. Double-joint PCR:
518 a PCR-based molecular tool for gene manipulations in filamentous fungi. *Fungal Genet*
519 *Biol* 41:973-981.
- 520 Zhang H, Kim M, Huang J, Shim W. 2017. FvLcp1, a novel LysM/Chitin-binding protein, is
521 important for ear rot virulence and fumonisin biosynthesis. *Phytopathology* 107: S5. 87
- 522 Zhang H, Mukherjee M, Kim JE, Yu W, Shim WB. 2018. Fsr1, a striatin homologue, forms an
523 endomembrane-associated complex that regulates virulence in the maize pathogen
524 *Fusarium verticillioides*. *Mol Plant Pathol* 19:812-826.
- 525 Zhang Z, Qin G, Li B, Tian S. 2014. Knocking out Bcsa1 in *Botrytis cinerea* impacts growth,
526 development, and secretion of extracellular proteins, which decreases virulence. *Molecular*
527 *Plant-Microbe Interactions* 27:590-600.
- 528 Zheng H, Zheng W, Wu C, Yang J, Xi Y, Xie Q, Zhao X, Deng X, Lu G, Li G, et al. 2015. Rab
529 GTPases are essential for membrane trafficking-dependent growth and pathogenicity in
530 *Fusarium graminearum*. *Environmental Microbiology* 17:4580-4599.
- 531 Zheng HK, Chen SM, Chen XF, Liu SY, Dang X, Yang CD, Giraldo MC, Oliveira-Garcia E, Zhou
532 J, Wang ZH, et al. 2016. The small GTPase MoSec4 is involved in vegetative development
533 and pathogenicity by regulating the extracellular protein secretion in *Magnaporthe oryzae*.
534 *Frontiers in Plant Science* 7.
- 535
- 536

537 **Figure legends**

538

539 **Fig. 1.** FvSec4 protein sharing high similarity with other fungal species. Protein sequence
540 alignment of *S. cerevisiae* Sec4, *F. verticillioides* FvSec4, *A. fumigatus* AfSrgA, *M. oryzae*
541 MoSec4. *C. lindemuthianum* CLPT1. White characters with black background and black
542 characters in a box indicate identical and similar sequences, respectively. Sec4 is predicted to have
543 six alpha helices and six beta strands.

544

545 **Fig. 2.** Vegetative growth of wild-type (WT), Δ Fvsec4, Δ Fvsec4-Com and Δ Fvsec4-GFP-FvSec4
546 (GFP) strains. (A) Strains were cultured on the V8, 0.2xPDA, myro agar plates for 8 days at room
547 temperature. (B) Δ Fvsec4 mutant enhanced hyphal branching compared to WT, Δ Fvsec4-Com
548 after 3 days on 0.2xPDA agar plates. Bar = 100 μ m

549

550 **Fig. 3.** Impacts of FvSec4 on conidia production (A) Conidia production in wild-type (WT),
551 Δ Fvsec4, Δ Fvsec4-Com strains were measured after incubation on V8 agar medium at room
552 temperature for 8 days. (B) Conidia germination rate in WT, Δ Fvsec4, and Δ Fvsec4-Com on
553 0.2xPDB were examined under microscope after 5 and 6.5h incubation with gently shaking. (C)
554 Mycelium fresh weight were assayed after 3-day incubation in YEPD liquid medium. (D)
555 Transcript differences of conidia-related genes in Δ Fvsec4 were compared to WT and Δ Fvsec4-
556 Com strains. Three biological replicates were performed independently. Error bars in this study all
557 represent the standard deviations for three replicates. Lowercase letters in this study on the bar top
558 suggest significant differences among various strains. (Student T-test, $P < 0.05$). All data in this
559 study were analyzed by Prism software.

560

561 **Fig. 4.** FvSec4 protein localization assay. (A) GFP-Sec4 protein driven by its native promoter
562 mainly localized to the apical area of growing hyphae. Bar = 5 μ m (B) Hyphal growth of wild-type
563 (WT), Δ Fvsec4, Δ Fvsec4-Com were examined under a microscope after 10 min of FM4-64
564 staining. The Spitzenkörper region in Δ Fvsec4 was compared with WT and Δ Fvsec4-Com. Bar =
565 5 μ m

566
567 **Fig. 5.** Role of FvSec4 in corn seedling rot severity. (A) We inoculated 10 μ l of wild-type (WT),
568 Δ Fvsec4, and Δ Fvsec4-Com spore suspension (10⁷/ml) on one-week old silver queen seedlings.
569 Symptoms were observed after 7 days of incubation. (B) Lesion sizes were quantified using Image
570 J.

571
572 **Fig. 6.** Influence of FvSec4 in FB1 production and key FUM gene transcription. (A) Surface
573 sterilized silver queen corn seeds were inoculated with wild-type (WT), Δ Fvsec4, Δ Fvsec4-Com
574 and incubated for 7 days. Sterile water was used as a negative control. (B) FB1 and ergosterol were
575 quantified by HPLC. Ergosterol level in each sample was used to normalize FB1 levels, thus
576 resulting in relative FB1 production in corn seeds. (C) Myro liquid medium was inoculated with
577 WT, Δ Fvsec4, and Δ Fvsec4-Com for 7 days at room temperature with agitation. FB1 levels were
578 analyzed by HPLC. (D) Transcriptional analyses of key FUM genes, exocyst-related genes, and
579 FvLcp1 in WT, Δ Fvsec4, Δ Fvsec4-Com after 7-day incubation in the myro liquid medium.
580 Transcripts were normalized against WT gene expression. Three biological replicates were
581 performed independently. Error bars in this study all represent the standard deviations for three
582 replicates. Lowercase letters in this study on the bar top suggest significant differences among
583 various strains.

584

585 **Fig. 7.** Susceptibility against cell wall stress agents and deficiency in carbon utilization in $\Delta Fvsec4$
586 mutant. (A) Strains were grown on Czapek-Dox agar amended with SDS, congo red and H_2O_2 for
587 8 days at room temperature. (B) Growth diameter of $\Delta Fvsec4$, $\Delta Fvsec4$ -Com were subjected to
588 statistical analyses. The growth inhibition rate (%) was measured by (sucrose growth diameter -
589 designated stress growth) / sucrose growth diameter x 100. (C) Strains were grown on modified
590 Czapek-Dox with dextrose, fructose or sorbitol as the sole carbon source for 8 days at room
591 temperature. Czapek-Dox agar plates with sucrose was used as a control. (D) Inhibition rate of
592 strains grown on the media containing different carbon sources. Three replicates were used in this
593 assay. The growth inhibition rate (%) was measured by (diameter of growth on sucrose - designated
594 carbon growth) / diameter of growth on sucrose x 100.
595

Fig. 1. Yan et al

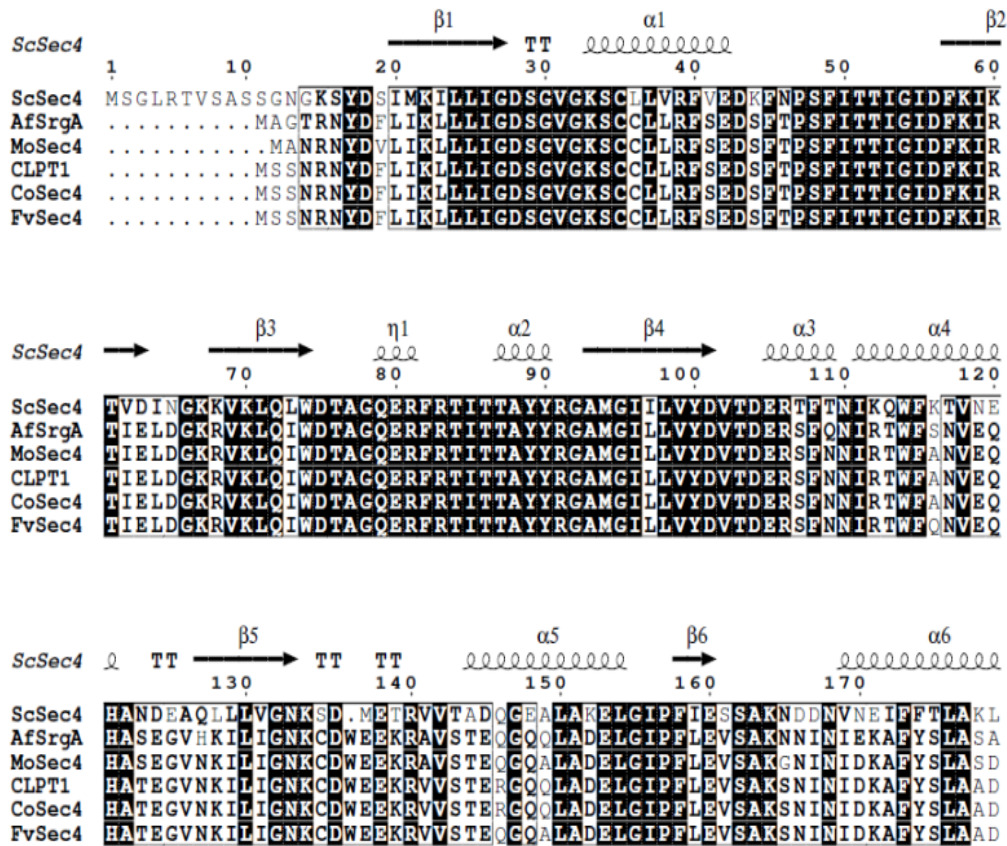


Fig. 2. Yan et al

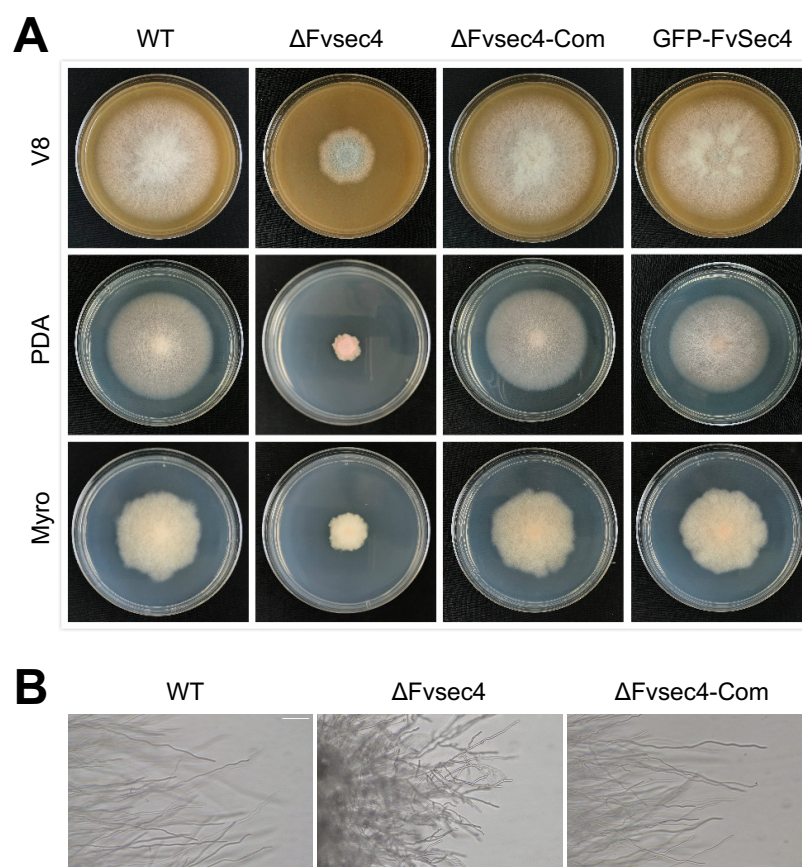


Fig. 3. Yan et al

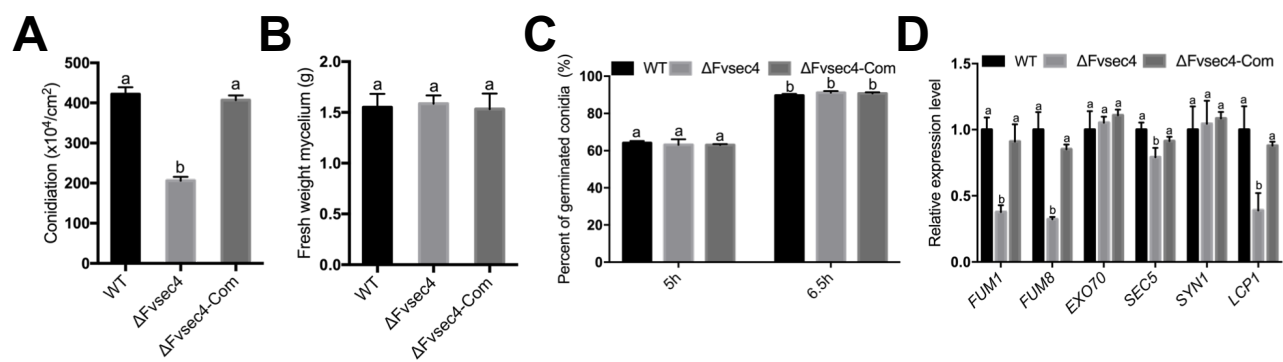


Fig. 4. Yan et al

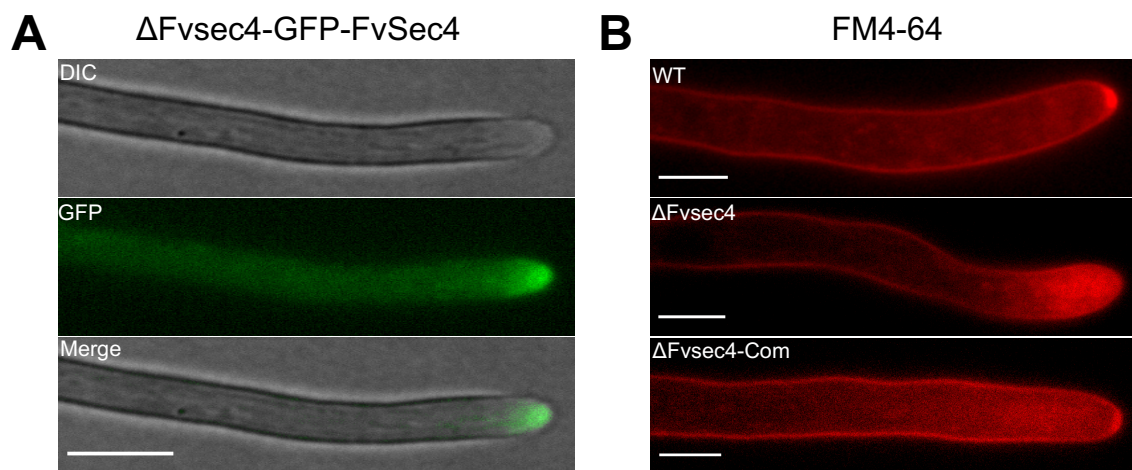


Fig. 5. Yan et al

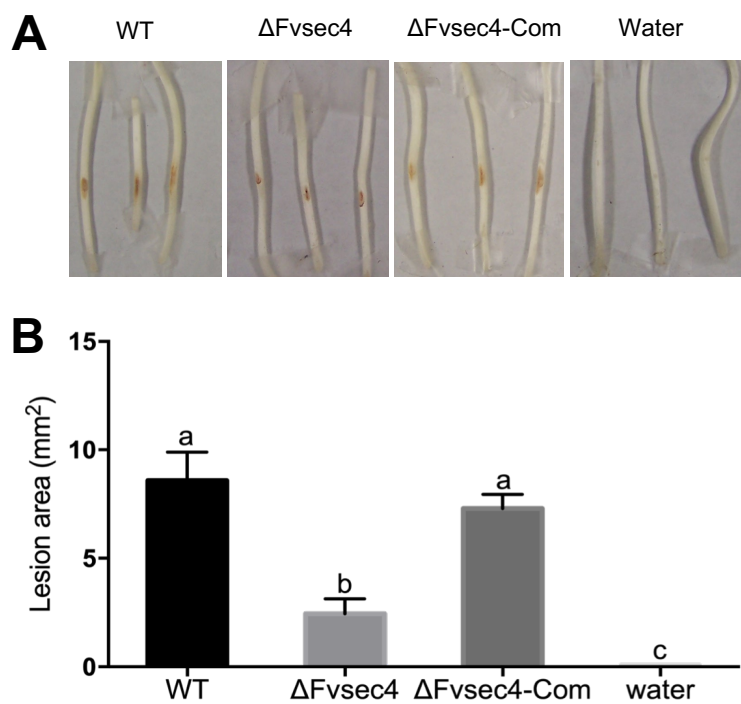


Fig. 6. Yan et al

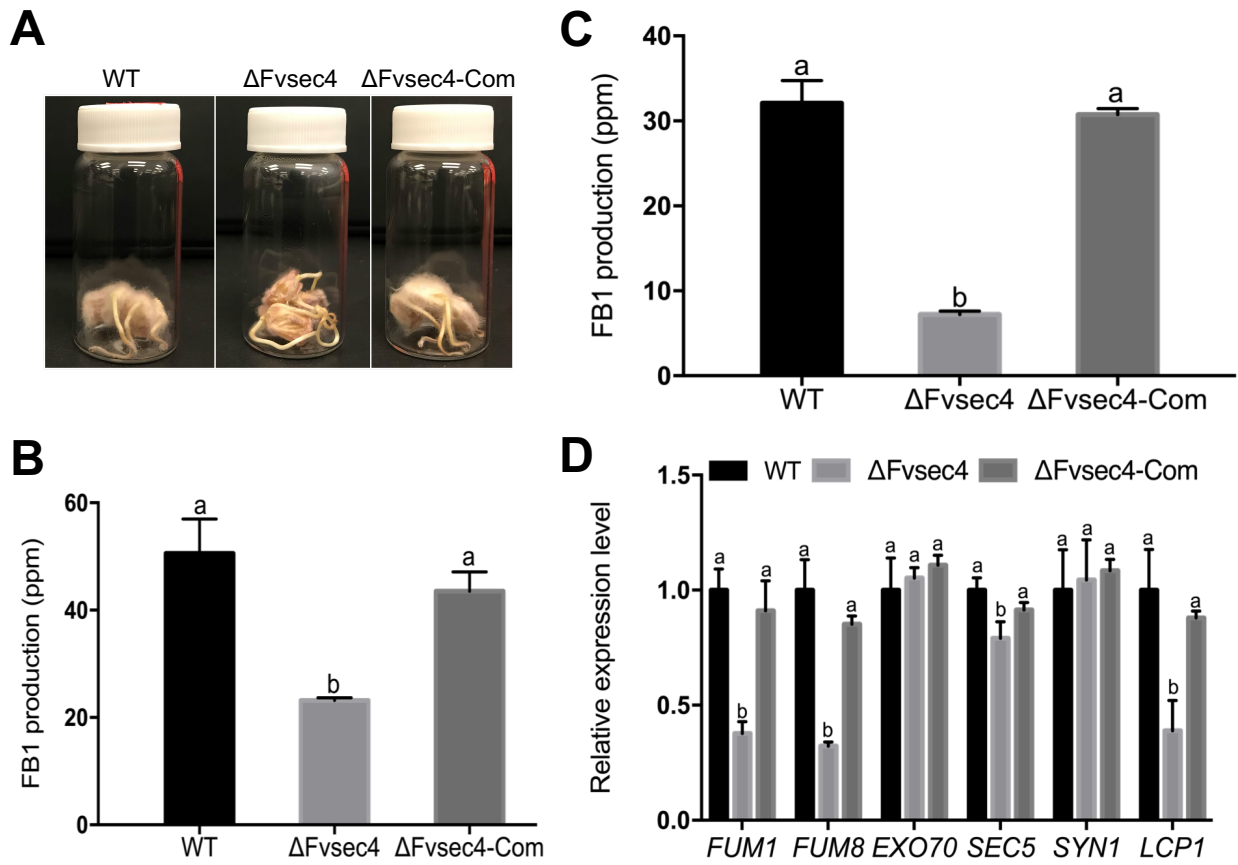
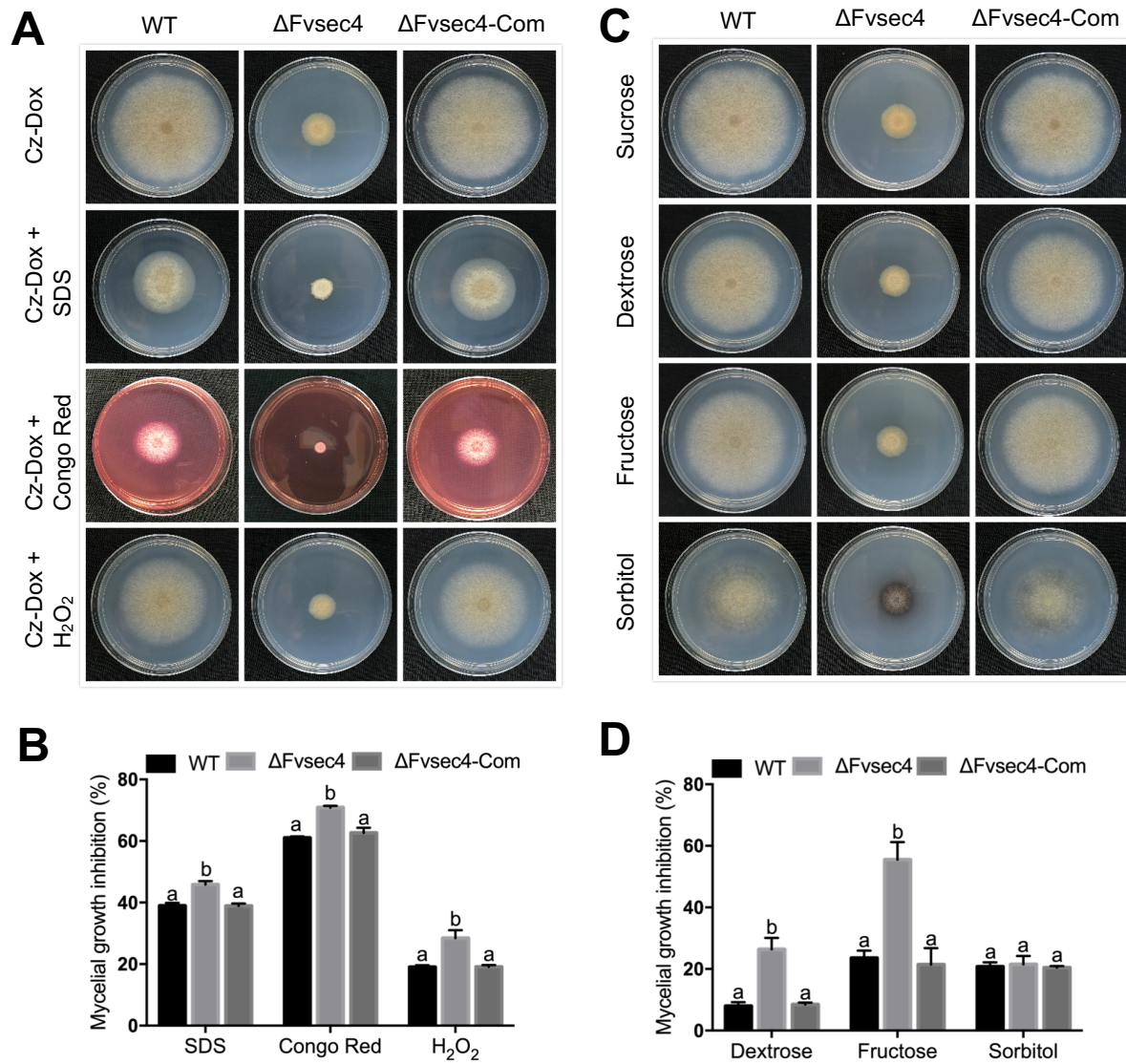


Fig. 7. Yan et al



Yan et al. Supplementary Information

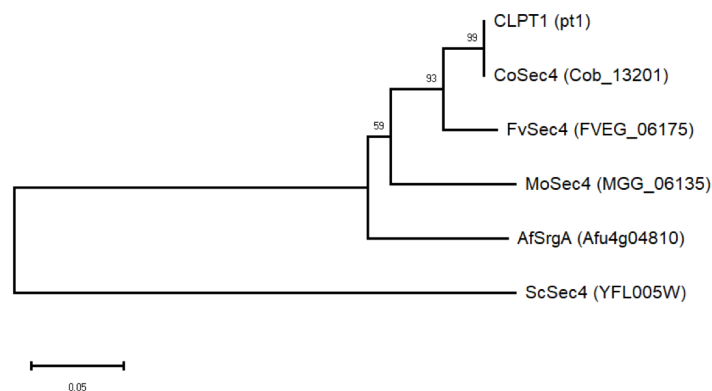


Fig.S1. (A) Phylogenetic analysis for FvSec4 and other Sec4 orthologs. Multiple sequences were aligned by ClusterX2. A neighbor-joining tree was constructed by MEGAX. The number at nodes indicates the percentage of replicate trees clustered together in 1000 bootstrap replications.

Yan et al. Supplementary Information

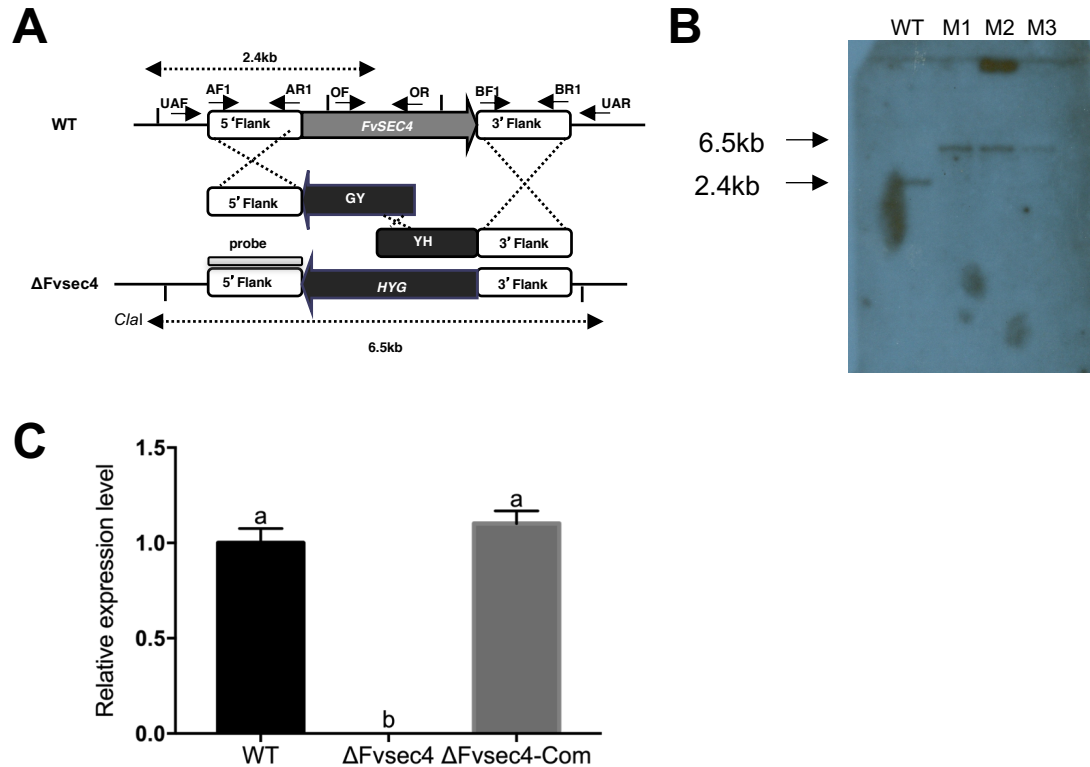


Fig.S2. (A) Homologous gene recombination approach used to construct $\Delta Fvsec4$ mutant in *F. verticillioides*. (B) Southern blot analyses of WT and three knockout candidates (M1, M2, M3). M1 was used in this study as $\Delta Fvsec4$. We used the 5'-flanking regions as a probe for Southern blot. (C) WT, $\Delta Fvsec4$ and $\Delta Fvsec4$ -Com total RNAs were isolated after 7 days in myro liquid medium and reversed to cDNA. qPCR was employed to verify the $\Delta Fvsec4$ and $\Delta Fvsec4$ -Com using a *FvSEC4* gene-specific primer set while WT was as a control. No detectable *FvSec4* transcript in the $\Delta Fvsec4$ mutant by qPCR analysis and $\Delta Fvsec4$ -Com fully recover the *FvSEC4* expression.

Yan et al. Supplementary Information

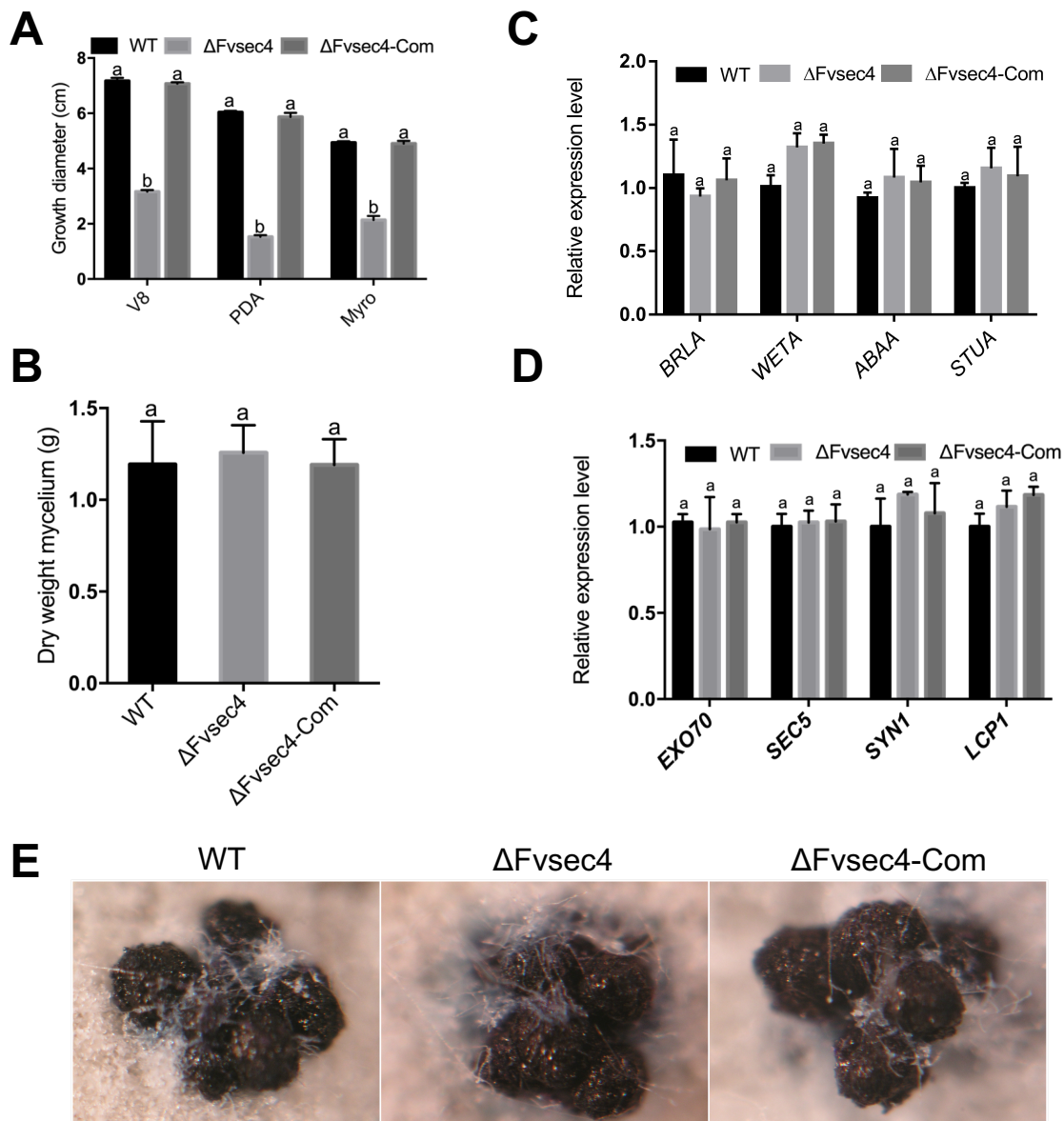


Fig.S3. Involvement of FvSec4 the vegetative growth but not perithecia in sexual mating. (A) Mycelia growth diameter on V8, 0.2xPDA and myro solid medium were assayed after 8 days at room temperature. (B) Same weight of mycelia from YEPD was transferred into myro liquid medium for constant shaking. Samples were collected after 7 days incubation in 100ml myro liquid medium. (C) qPCR study of *BRLA*, *WETA*, *ABAA* and *STUA* after 20 h incubation in YEPD liquid medium (D) 20 h samples in YEPD medium was studied the expression of exocyst-related and FvLcp1 gene expression. (E) WT, $\Delta Fvsec4$ and $\Delta Fvsec4$ -Com were crossed to M3120, an opposite mating type to assay fertility.

Table S1. Primers used in this study

Primer	Primer sequence (5'-3')	Application
UAF	TTC CTG CTC CCT ATG GTG AT	amplify <i>FvSEC4</i> 5' flank sequence
AF1	GTG AAT GTG GTT GCC AGA ATG C	<u>amplify <i>FvSEC4</i> 5' flank/probe sequence</u>
AR1	<u>TAG ATG CCG ACC GGG AAC</u> CGGGACTAATCCGTTTGC	<u>amplify <i>FvSEC4</i> 5' flank/probe sequence</u>
BF1	<u>CCA CTA GCT CCA GCC AAG AGC</u> GGT CGT TGT TGG AGT A	<u>amplify <i>FvSEC4</i> 3' flank sequence</u>
BR1	CTC TTG ACC CGA TAC CTA ATC G	amplify <i>FvSEC4</i> 3' flank sequence
UAR	GCC CTT CCT CCC TTT ATT TC	amplify <i>FvSEC4</i> 3' flank sequence
HYG/F	TTG GCT GGA GCT AGT GGA GGT CAA	amplify HY fragment
HY/R	GTA TTG ACC GAT TCC TTG CGG TCC GAA	amplify HY fragment
HYG/R	GTT CCC GGT CGG CAT CTA CTC TAT	amplify YG fragment
YG/F	GAT GTA GGA GGG CGT GGA TAT GTC CT	amplify YG fragment
OF	AAT CGC ATC GCA CTG TTG TC	<i>FvSEC4</i> ORF screening
OR	AGC GCA TTG CTT TGT TGG	<i>FvSEC4</i> ORF screening
AF2	TCA AGT ATC CCA TGC CAG TTC	<u><i>FvSec4</i> complementation</u>
BR2	TGG CTG AGG GCT TTG GTT	<u><i>FvSec4</i> complementation</u>
SEC4-PF	<u>GTC GAC GGT ATC GAT AAG CTT</u> TCA AGT ATC CCA TGC CAG TTC	amplify <i>FvSEC4</i> promoter sequence
SEC4-PR	<u>CTC GCC CTT GCT CAC CAT</u> GTT GAC CAA GAG TGA GAG TAG C	amplify <i>FvSEC4</i> promoter sequence
GFP-F	ATG GTG AGC AAG GGC GA	amplify GFP sequence
GFP-R	CTT GTA CAG CTC GTC CAT GC	amplify GFP sequence
ORF-F	<u>CAC GGC ATG GAC GAG CTG TAC AAG</u> ATG TCG AGT AAT CGC AAC TAT GAT	amplify <i>FvSEC4</i> cDNA sequence

ORF-R	<u>GGA CTC CTT AGG GTA TTC GGT</u> TTA GCA GCA CTT GCT	amplify FvSEC4 cDNA sequence
Ter-F	ACC GAA TAC CCT AAG GAG TCC	amplify <i>FvSEC4</i> terminal sequence
Ter-R	<u>TCA GTA ACG TTA AGT GGA TCC</u> TAT GAC GGA GGA GAC GAG GT	amplify <i>FvSEC4</i> terminal sequence
FvBrlA-qpcr-F1	CGT CAC AAG CAA ACT TTC CAC GGT	qPCR analysis
FvBrlA-qpcr-R1	CGT GTA GCT TGC GGT GGT TGT T	qPCR analysis
FvwetA-qpcr-F1	GGC ATC CAC ACA CCA GCA GAA T	qPCR analysis
FvwetA-qpcr-R1	GAT GCT GCC AAG CTG ACT GAG GA	qPCR analysis
FvAbaA-qpcr-F1	TAC CGC AAC CGA CAA GCA CAC AA	qPCR analysis
FvAbaA-qpcr-R1	GTG AGG CAT GAG AAG AAC AGA GTC AAC A	qPCR analysis
FvStuA-qpcr-F1	TGT AGC ACG GAG AGA AGA TAA CCA CAT GA	qPCR analysis
FvStuA-qpcr-R1	ATC TTG ACG ACG TGG CGA ACC TTT	qPCR analysis
FvEXO70-qpcr-F1	GCT CTA GAT GAA GAA GCA AGG GCT GA	qPCR analysis
FvExo70-qpcr-R1	ATC AAC GTT ATT TCC CAA TAT CTG CAG TCG	qPCR analysis
FvSec5-qPCR-F1	TGA AGA AGA CGG AGG ACG ACT GGT TAA T	qPCR analysis
FvSec5-qPCR-R1	CGA ATG TTT CTA TCC CCT GAG TCC AAT GC	qPCR analysis
Syn1-qpcr-F1	CCC TCG TCG TTC AGC AAG AA	qPCR analysis
Syn1-qpcr-R1	AGC AAC ACA AAT ACC CAA GCA G	qPCR analysis
Lcp1-qpcr-F1	TAT GGA CCT GAG GAG GAC GAA TG	qPCR analysis
Lcp1-qpcr-R1	CAC CAA AGG TAC TCC CAG CAA TC	qPCR analysis
FVEG_Sec4_qPCR_F1	GTG CGA CTG GGA GGA GAA GCG	qPCR analysis
FVEG_Sec4_qPCR_R1	GCT GAG GGT TGG TCG TTC TTG G	qPCR analysis
Tub2-F	CAG CGT TCC TGA GTT GAC CCA ACA G	qPCR analysis
Tub2-R	CTG GAC GTT GCG CAT CTG ATC CTC G	qPCR analysis